Effect of DMDBS (3 : 2, 4-bis(3,4-dimethyldibenzylidene) sorbitol) and NA11 (sodium 2,2′-methylene-bis(4,6-di-tertbutylphenyl)-phosphate) on Electret Properties of Polypropylene Filaments

Ali Kilic, Eunkyoung Shim, Bong Yeol Yeom, Behnam Pourdeyhimi

The Nonwovens Institute, North Carolina State University, 2401 Research Drive, Campus Box 8301, Raleigh, North Carolina 27695

Correspondence to: E. Shim (E-mail: eshim@ncsu.edu)

ABSTRACT: Polypropylene (PP) composite filaments containing two different nucleating agents—DMDBS (3 : 2, 4-bis(3,4-dimethyldibenzylidene) sorbitol) and NA11 (sodium 2,2′-methylene-bis(4,6-di-tertbutylphenyl)-phosphate) were melt spun to modify polymer electrostatic charging characteristics. Sample filaments were charged with a corona instrument and their surface potentials were measured. Initial surface potential as well as potential stability was monitored through an accelerated decay procedure. NA11 was found to be more efficient as an electret additive leading to a 50% increase in charge stability. Filaments with DMDBS exhibited a faster decay. Charging at elevated temperatures resulted in enhanced charge density and stability for both additives. The fiber microstructure was examined by Wide Angle X-ray Diffraction and Differential Scanning Calorimetry. Rather than reducing the crystal sizes, X-Ray diffractograms suggest that the crystal size increases with the addition of nucleating agents, while the degree of crystallinity appears to remain unaltered. © 2013 Wiley Periodicals, Inc. J. Appl. Polym. Sci. 000: 000–000, 2013

INTRODUCTION

Due to their quasi-permanent charging property, electret materials are useful in various applications. Early pioneers Sessler and West[1] used metalized fluoropolymer electrets to develop microphones. Instruments were designed to analyze the concentration of energetic ions that spread from radioactive sources.[2] Over the past few decades, electret filters have attracted significant attention due to their high filtration efficiency at reduced pressure drops. Among these, filters that are electrostatically charged have gained significant interest in recent decades.

There are two main approaches to improving filtration efficiency. One approach is the use of finer fibers, which leads to increasing mechanical capture efficiencies. They separate particulates from air streams through well-known mechanisms of impaction, interception, and Brownian diffusion. However, the use of fine fibers will also potentially result in a higher pressure drop. A second approach is electrostatically charging the filtration medium. In this type of filters which referred to as "electret filters" or "electrostatic filters,"[3] electrostatics offer as fourth mechanism that is quite effective for capturing sub-micron particles.[4,5] Electret filters are advantageous over mechanical filters due to their low pressure drop since it does not requires

alteration of the web structure to achieve high filtration efficiencies. It is not, therefore, surprising that electrostatic filters are used in high efficiency filtration because they are effective at lower pressure drops which can lead to energy savings in HVAC systems.

Since electret filters rely mainly on particle electrostatic attraction for capture, they use loosely packed webs, composed of coarser fibers leading to lower pressure drops. However, not all electret filters have high electret efficiency. In other words, commercial filters possess varying levels of electrostatic charge. It is also known that the instability of the charge and its potential loss may result in much reduced capture efficiencies. As an example, for HVAC systems installed at a hospital, Raynor et al.[6] observed that the filtration efficiency for particles around 0.3–0.5 μm dropped to below 50% in only 5–6 weeks after installation.

While many nonwoven production processes produce triboelectrically charged webs, the charging density is not high and the charge stability is rather poor. Therefore, it is common to employ additives during the extrusion process and use a charging step after the web is formed to attain high charge density and improved stability.

Over the last decade or so, many "electret additives" have been studied by various researchers for enhancing the charge density and stability of electret filters. This is because the use of high dielectric constant additives changes the polarization properties of host polymers, such as polypropylene (PP).[7] Note that high initial charge density does not necessarily imply high stability; a major reason for the loss of charge in filters is due to the formation of a conductive liquid film during filtration.[8–12] It is not therefore, surprising that fluorochemicals in the form of a mist have been applied to webs to resist the formation of a conductive film. In addition to dielectric additives, it has been determined that nucleating agents are useful for improving the electret properties of PP films.[13–20] The addition of nucleating agents results in smaller crystal size whose boundaries act as potential traps for space charges.[14] Space charge formation in a dielectric body is known as the Maxwell–Wagner effect which is attributed to material discontinuities. Maxwell showed that charges will accumulate in time at the interfaces between the layers whenever $\varepsilon_1\sigma_1 \neq \varepsilon_2\sigma_2$ (where ε and σ indicates dielectric constant and conductivity, respectively).[21] On the other hand, non-soluble nucleating agents can create micro-voids, which are believed to prohibit charge migration in film electrets.[13]

Bisamides,[15] trisamides,[14,20] sodium 2,2′-methylene-bis(4,6-di-tert-butylphenyl)phosphate (NA11),[15,17] and N,N′-dicyclo-hexyl-2,6-naphthalene-dicarbox-amide (NU100)[16] are among the nucleating agents that have been examined. The effect of isomer and the length of alkyl chain was examined on low molecular weight 1,4-phenylene bisamides as β-crystal nucleators with different substituents. Bisamides containing long aliphatic side chains disturbed the nucleation ability, so as charge stability of PP films. Varying the symmetry of the additive molecules also resulted in changes in electret properties, but the concentration had a more prominent impact on charge stability. Comparing with the remaining potential after annealing at 90°C for 24 h, approximately a 20% improvement was achieved for PP films containing bisamide additives at concentrations below 0.05 wt %. At higher concentrations, electret properties dropped, not only because of network formation but also due to percolation of insoluble additive aggregates in the system.[18]

Similarly, the addition of triphenylamine based trisamides at higher concentrations (0.04 wt %) introduced charge carriers at sufficient quantities to cause noticeable conductivity.[14] A comparison of trisamides comprising amide groups and cyclohexyl substituents showed that the presence of –NH groups resulted in self-assembly, thus formed macrodipoles which gave rise to charge retention. Trisamides without those amide groups exhibited worse stability even compared to pure films. Larger 3D network structures were observed at higher concentrations which possibly led to percolation. Higher initial potentials could be reached around percolation concentration, but it decayed rapidly.[20]

On the other hand, NA11 and some nucleating agents that not dissolve in PP may form micro-void during the film formation process. Their electret characteristics were thought to be depending on formation of elongated voids which could potentially act as charge barriers against decay. Upon stretching, the
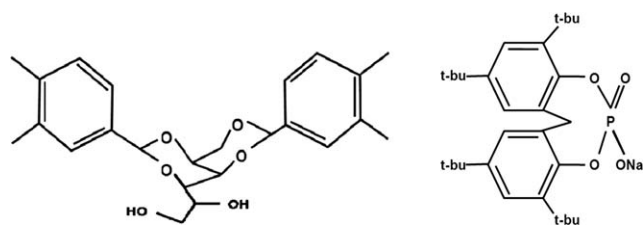

Figure 1. Chemical formula of DMDBS (left) and NA11 (right).

effect of formed cavities becomes more dominant for films containing NA11 resulting in improved stability.[15,17]

Previous studies dealing with the electret effects of nucleating agents were focused on metallized PP films. It may not fully explain charging behavior of electric filter media, which consist of assembly of fibers. It is well known that fiber spinning process create different polymer fine structures. In addition, surface area of fiber based system is far greater than film based system. In this study, the morphological and electret characteristics of non-metalized round PP filaments containing nucleating agents was investigated to explore the suitability of nucleating agents for enhancing electret properties of aerosol filtration media. Below, we report on two different nucleating agents, a soluble sorbitol based DMDBS and a non-soluble organophosphorous compound, NA11.

EXPERIMENTAL

Sample Preparation

PP resin (grade CP36OH, density = 0.91 g cm^{-3}, Melt flow index = 34 dg min^{-1}), with a weight average molecular weight of 180,000 g mol^{-1} and a polydispersity of 3.3 was supplied by Sunoco Chemicals (PA). DMDBS and NA11 in powder form were obtained from The Milliken Company (SC) and BASF (NJ), respectively. Figure 1 shows the molecular structures of the additives used.

Masterbatch pellets at a concentration of 20% (w/w) concentration were prepared by Techmer PM (TN). From this masterbatch, PP filaments containing additives at 0.1, 0.5, 1, and 5% concentrations were melt-spun in the multifilament extrusion facility located in the Nonwovens Institute (North Carolina State University, Raleigh). The filament spinning speed was 2000 m min^{-1} and the throughput per capillary was maintained at 0.58 g hole^{-1} min^{-1}. As control, PP filaments without any additives were also melt extruded under identical conditions. Each filament bundle had 72 filaments, and each filament has diameter of ~20 μm.

All samples were washed with deionized water at 45°C for 6 h to remove any potential impurities as well as the spin finish applied during melt spinning. The washing fluid was replaced every 2 h. The filaments were wound on washing tubes and dried overnight.

Fiber Structure Analysis

Microscopy. Optical microscopy images were obtained to determine the dispersion of additives within the PP filament. A Zeiss optical microscope with an objective of 40× was used and images were captured with a Nikon high-definition color

camera, DS-Fi1 mounted on the microscope. To validate the observations of the optical micrographs with respect to particle distribution within filament cross-section, SEM analyses were performed. A Hitachi S-3200 Scanning Electron Microscope equipped with a tungsten filament to create the beam was used. The reported resolution was 35 Angstroms with a 30 kV beam. A 30 μm diameter objective aperture and a 25 mm working distance were used for imaging. To avoid any damage to the cross-section, sample filaments were cut with a razor blade in liquid nitrogen which is well below glass transition of PP.

Differential Scanning Calorimetry (DSC). The melting and crystallization behavior of the composite were analyzed by using a Perkin-Elmer differential scanning calorimeter. Samples weighing 4.0 $\pm$ 0.5 mg were heated in a nitrogen atmosphere from 25°C to 190°C at a rate of 20°C min^{-1}. During each run, the sample was kept for 4 min at the highest temperature prior to cooling in order to ensure complete melting of the polymer and remove any thermal history. Crystallization and melting temperatures reported here correspond to the peak temperatures in the DSC thermograms. Also, the crystallinity of the samples was calculated by using the following formula:

$$\% \text{ Crystallinity} = \frac{\Delta H}{\Delta H_{PP}^0} \times 100 \tag{1}$$

where, ΔH is the enthalpy of fusion of the sample (J g^{-1}) and ΔH_{PP}^0 is the enthalpy of fusion of completely crystalline PP ($\sim$207 J g^{-1}).[22]

Wide Angle X-ray Diffraction (WAXD). The crystal structure of the samples was evaluated by using an Omni Instrumental X-ray diffractometer. The diffractometer is equipped with a Be-filtered Cu $K\alpha$ radiation with a wavelength of 1.54 Å generated at 35 kV and 25 mA. The filament samples were wounded on the sample holder and the placed in the sample camber. The samples were scanned from 2θ range from 10° to 30° at an increment of 0.1°.

The crystal sizes of the samples were calculated by using the Scherrer equation.[23]

$$t = \frac{0.9\ \lambda}{B\cos\theta_B} \tag{2}$$

where, t Crystal size (Å); λ Wavelength of X-ray (1.54 Å); B Full Width at Half Maximum (radian); θ_B Bragg angle (degree)

Charging and Characterization of Charging Property
The filament bundles were aligned parallel on aluminum sample holders with a definite spacing (10 filament bundle cm^{-1}) as shown in Figure 2. Fibers protruding from the prepared specimen can cause significant variations in the value of potential measured. Thus, perpendicular filament bundles were aligned at a distance of 0.7 cm from one another. The filaments were fixed carefully by using a conductive tape and epoxy to prevent errors that can occur due to position changes during charging and decay tests.

A point-to-plate negative corona discharger (Mystic Marvels, Model NIP-7E) was used to charge the samples. The applied
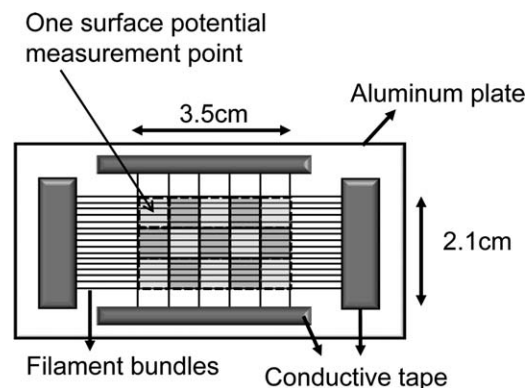

Figure 2. Schematics of a Specimen prepared for charging and surface potential analysis. Horizontal and vertical lines represent sample filament bundles aligned. Filaments were aligned parallel with the spacing of 10 filament bundles per cm to the horizontal direction first and additional filament bundles were aligned perpendicular to them with the spacing of 0.7 cm. Each rectangle represents one surface potential measurement points. Total of 15 points per each specimen was measured.

voltage was set at 9 kV where the maximum output direct current of the emitter needle was $\sim$160 μA. The charging time was kept constant for 1 min. The charging procedure was performed at a relative humidity of 54–58% RH and at a temperature of 22–23°C for "cold" charging. For "thermal" charging, samples were heated to 130°C, which took approximately 15 s, then charged for 1 min, and cooled down to room temperature.

The surface potential was measured with a Monroe Model 244A non-contact electrostatic voltmeter. Three specimens were prepared from each sample and the surface potentials of 15 specific points across each specimen were measured. The data reported are the average and the standard error of a total of 45 points. The initial potential value (V_0) was measured directly after charging. Charge stability was evaluated according to the isothermal surface potential decay (SPD) test.[24] Charge dissipation or depolarization of the polymer electrets may take as long as several years.[25] Therefore, we performed decay tests at elevated temperatures to accelerate the charge decay process. Charged samples were placed in the oven at 80°C and their surface potential was measured after 0.5, 1, 2, 4, 8, 12, 16, and 24 h decay time. Samples after annealing were cooled for 10 min in a desiccator to ensure there were no influences from the atmosphere.

RESULTS

Fiber Structure
The distribution of additives was investigated by optical microscopy. For the miscible DMDBS, no varying phases were observed under visible light, whereas the solid NA11 particles produced elongated cavities. Optical images of samples containing 1 and 5% NA11 are shown in Figure 3.

The formation of cavities would be an indicator of early solidification. As indicated in Figure 4, the surface also appears to have become rougher with the addition of NA11.
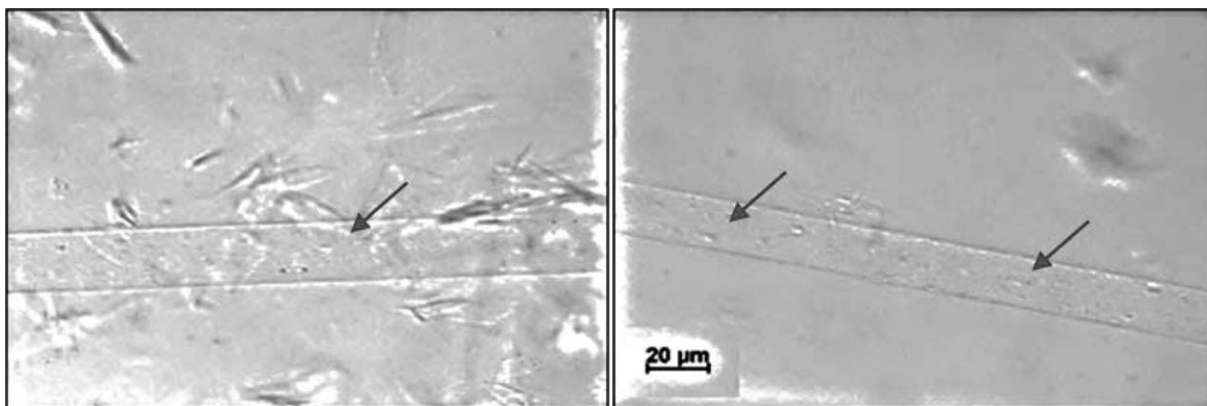
Figure 3. Optical micrographs for samples containing 1% NA11 (left), 5% NA11 (right). Arrows indicate elongated cavities.

It is known that the addition of nucleating agents may change the polymer microstructure, i.e., crystal forms and size.[26] In Figure 5(b), there appears to be a substantial increase in the crystallization temperature of samples containing nucleating agents. As expected, the melting temperature remained unchanged around $160 \pm 2°C$ for both the control and sample containing nucleating agents [Figure 5(a)]. The difference in melting (T_m) and crystallization temperatures (T_c) of DMDBS/PP and NA11/PP filaments was determined from the DSC cooling results (Figure 6). At a cooling rate of 20°C/min, there appears to be a significant increase in the crystallization temperature (T_c) as a result of the addition of nucleating agents. NA11 appears to cause such a change at 0.1% concentration, whereas DMDBS/PP shows such an effect at 0.5% concentration.

X-Ray diffractograms of samples containing 0.5 and 5% additive are given in Figure 7. Peak intensities increased at low concentrations, which indicate clear PP crystals. At higher
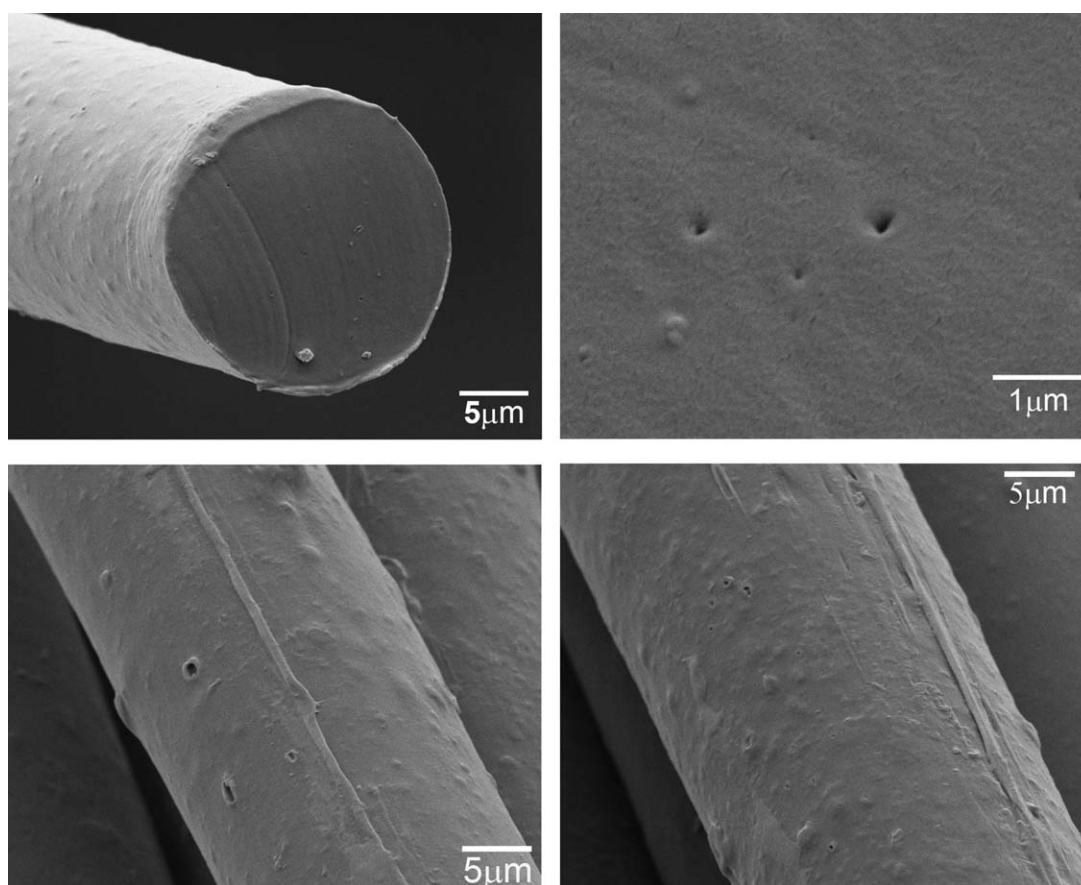

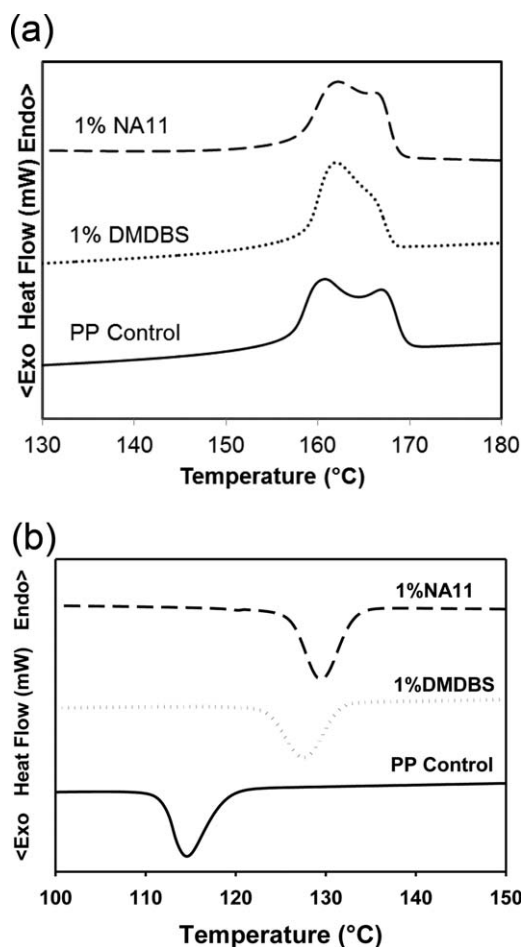**Figure 4.** SEM images of fibers containing 5% NA11.

Figure 7. Wide-angle X-ray diffractograms of PP filaments containing nucleating agents.

obtained at a 1% concentration of nucleating agents. This is in agreement with earlier findings for films.[26]

Table I summarizes the analysis of WAXD data for the control and samples containing nucleating agents. All samples exhibited characteristic peaks of α-polypropylene crystal. However there are minor differences in 2θ values which would indicate differences in d-spacing.

From the DSC thermograms, crystallinity values of the filaments were calculated (Figure 9). For both additives, at concentrations below 1%, the crystallinity appears to be unchanged in comparison with that of the control. At a concentration of 5% for DMDBS, the crystallinity appears to be lower, whereas a notable increase was observed with NA11 at the same concentration.

Charging Properties
As shown in the isothermal potential decay graphs (Figure 10), samples containing DMDBS exhibited a faster decay, compared

Figure 5. (a) Heating and (b) cooling DSC thermograms of the PP control and filaments containing 1% nucleating agents.

concentrations, peaks became wider, similar to control sample. From the DSC results, it appears that the addition of nucleating agents results in faster crystallization. This can lead to longer time for crystal growth. The change in the crystal sizes for (110) plane is summarized in Figure 8. The largest crystals were
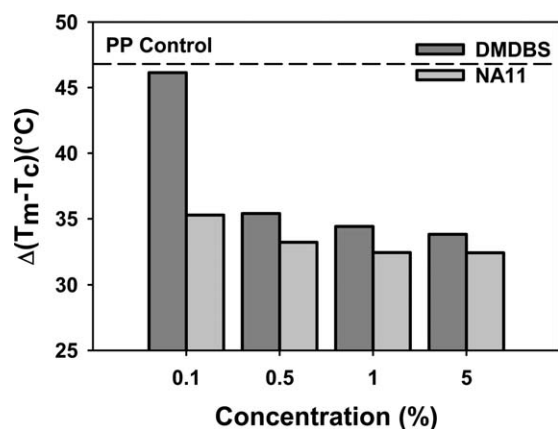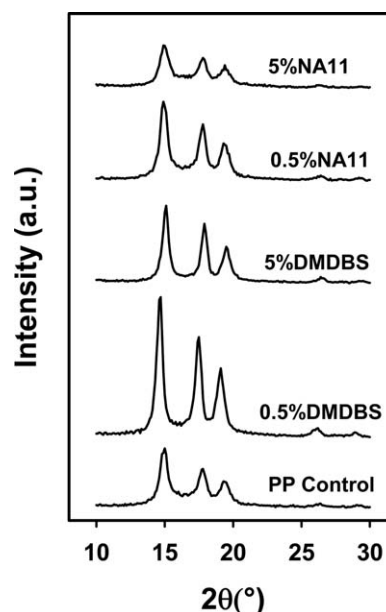

Figure 6. The difference between melting and crystallization temperatures, $\Delta(T_m - T_c)$ of samples containing different nucleating agents. A dotted line represents the value of the PP control sample.
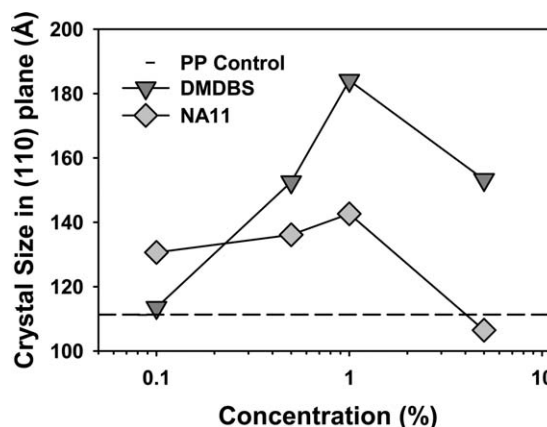

Figure 8. Crystal size in (110) planes of PP fiber containing nucleating agent. A dotted line represents the crystal size of the PP control sample.

Table I. Detailed WAXD Analysis for Various Nucleating Agent Concentrations

Additive concentrations (%)	2θ (°)	Size (Å)	Possible crystal structure
0	14.99	111.2	α-Polypropylene(1,1,0)
	17.73	144.8	α-Polypropylene(0,4,0)
	19.40	112.0	α-Polypropylene(1,3,0)
0.1% DMDBS	14.88	113.5	α-Polypropylene(1,1,0)
	17.65	114.6	α-Polypropylene(0,4,0)
	19.32	124.6	α-Polypropylene(1,3,0)
0.5% DMDBS	14.60	152.5	α-Polypropylene(1,1,0)
	17.46	155.0	α-Polypropylene(0,4,0)
	19.06	124.1	α-Polypropylene(1,3,0)
1% DMDBS	14.66	184.0	α-Polypropylene(1,1,0)
	17.48	210.9	α-Polypropylene(0,4,0)
	19.12	131.4	α-Polypropylene(1,3,0)
5% DMDBS	15.07	153.3	α-Polypropylene(1,1,0)
	17.88	208.1	α-Polypropylene(0,4,0)
	19.51	125.8	α-Polypropylene(1,3,0)
0.1% NA11	15.43	130.6	α-Polypropylene(1,1,0)
	17.80	144.0	α-Polypropylene(0,4,0)
	19.46	120.6	α-Polypropylene(1,3,0)
0.5% NA11	14.96	136.1	α-Polypropylene(1,1,0)
	17.74	138.5	α-Polypropylene(0,4,0)
	19.39	119.9	α-Polypropylene(1,3,0)
1% NA11	14.96	142.6	α-Polypropylene(1,1,0)
	17.75	127.6	α-Polypropylene(0,4,0)
	19.40	115.2	α-Polypropylene(1,3,0)
5% NA11	15.01	106.5	α-Polypropylene(1,1,0)
	17.76	130.2	α-Polypropylene(0,4,0)
	19.41	105.9	α-Polypropylene(1,3,0)

to control samples at all concentrations in the range of 0.1 to 5%. At 0.1% concentration, the initial surface potential was high, but was accompanied with rapid charge decay. On the
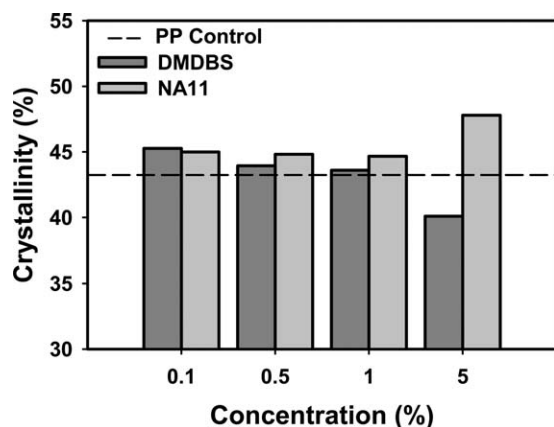
Figure 9. Crystallinity of nucleating agents/PP filaments calculated from DSC thermograms.

other hand, samples containing NA11 exhibited better charging properties when compared to control PP. Particularly at 5% concentration, the increase in initial potential and charge stability appears to be significant.

The initial electret filtration efficiency will be dependent on the strength of the field generated within the webs, which corresponds to the initial potential values of filaments. In time, charge decay will result in a reduction in capture efficiency. The charge decay behavior can be further described by an exponential decay. The relaxation time corresponds to 1/eth value of initial potential and is calculated according to:

$$V = V_0 e^{-t/\tau},\qquad(3)$$

where, V is surface potential measured at the decay time t, V_0 is initial potential, and τ is relaxation time.

Relaxation time (τ) which corresponds to the 1/eth value of the initial potential can used to evaluate charge stability of modified filaments. Figures 11 and 12 show the initial absolute potential and relaxation times of the corresponding samples. The initial potential values are close to that of the reference filaments containing nucleating agents. On the other hand, the charge decay in samples containing DMDBS is significantly faster. Interestingly, both the initial potential and the charge stability of sample containing 1% NA11 are significantly low. This confirms the observations by Hillenbrand et al. for PP films.[17] However, the effect was not so destructive in their case.

We know that interfacial polarization takes place in heterophase systems where there are boundaries between phases of different conductivity and permittivity.[27] Thus, polarizability of the samples would be enhanced when the crystals are smaller; smaller crystals will produce comparatively larger interfaces in total, where space charges are located. Additions of DMDBS resulted in larger crystal sizes (Table I) and lower crystallinity at higher concentration. This may partially explain reductions of initial surface potential and charging stability of these samples (Figure 9). Effects of NA11 on crystalline structures are different from those of DMDBS. Both crystalline and crystallinity slightly increases which would not negatively affect charging properties. In addition, the interfaces will also be built-up between the polymer and nonsoluble NA11additive and it would improve charge stabilty.

Charging Properties after Thermal Corona Discharge
It is well known that more stable electrets would be possible via thermal charging. Improved corona conditions and activation of polarizable species due to enhanced charge carrier mobility at elevated temperatures would be reasons behind this phenomenon.[3,28]

Therefore, we charged the samples for 1 min at 130°C, which is the maximum temperature we can achieve without damaging the fibers in our system. Resultant electret properties of samples containing both DMDBS and NA11 were significantly different from those obtained for the cold charged samples (Figure 13).

Thermally charged samples containing NA11 at 0.5 and 5% concentration exhibited longer charge stability when compared to DMDBS. Interestingly, samples containing DMDBS at 5%
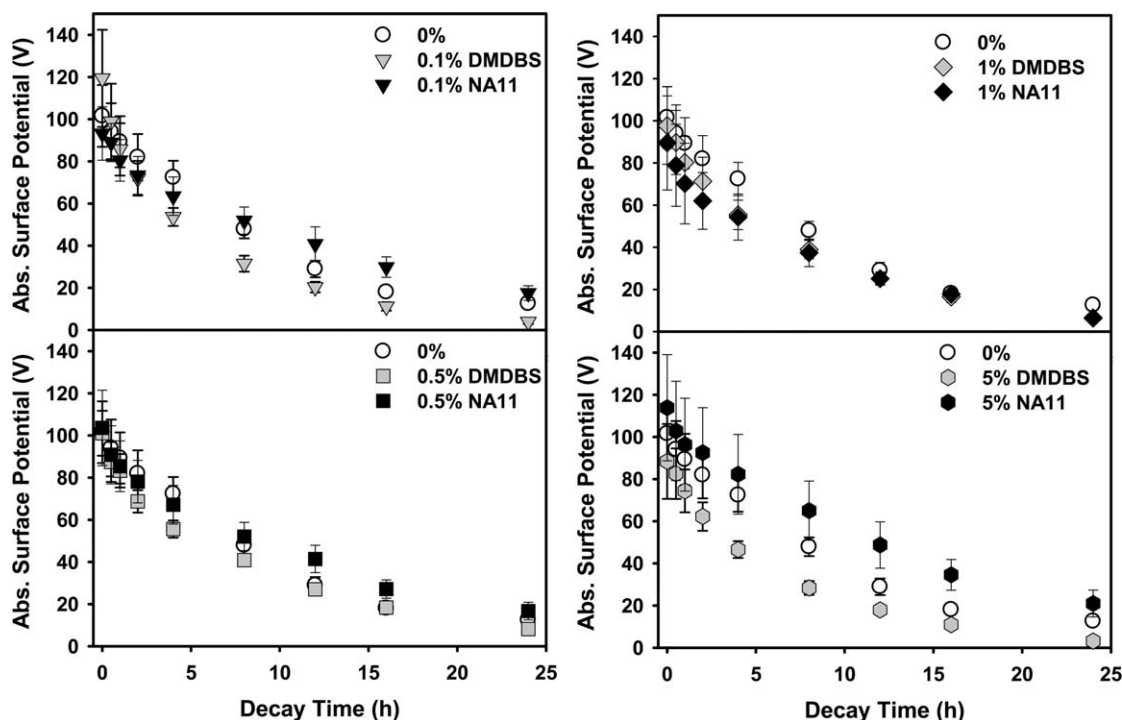
Figure 10. Isothermal surface potential decay (ISPD) of cold charged DMDBS/PP and NA11/PP filaments (charging time 1 min).

was found to be more stable and highly charged compared to the reference sample, whereas initial surface potential was significantly low for 0.5% DMDBS/PP sample. On the other hand, as shown in Figure 13, the initial surface potential of cold charged samples was similar for the control and NA11/PP filaments, whereas it was almost doubled for thermally charged samples containing NA11. Regardless, the relaxation times were higher for all modified samples.

DISCUSSION

Samples containing DMDBS did not improve charge stability at any concentration upon cold charging. However, at 5% concentration, both additives had significantly longer stability when thermally charged. Like bisamides and trisamides, which are

forming conductive aggregates, stability of samples containing DMDBS was expected to get worse due to percolation concentration resulting from H-bond formation.[18–20] Probably, the high shear rates during extrusion did not allow such drift pathways and dispersed DMDBS aggregates uniformly within the filaments.

For films containing NA11, elongated voids are thought to be acting as barriers against charge drift[11] through electrodes. The incorporation of polar groups into a nonpolar PP should be dominating the electret properties. The species, which have increased total polarizability of modified samples, provided higher performance after thermal charging. Due to the nature of orientational polarization, high temperature would lead to higher molecular mobility. This is a higher initial potential was obtained for filaments containing 5% DMDBS and 0.5 and 5% NA11.
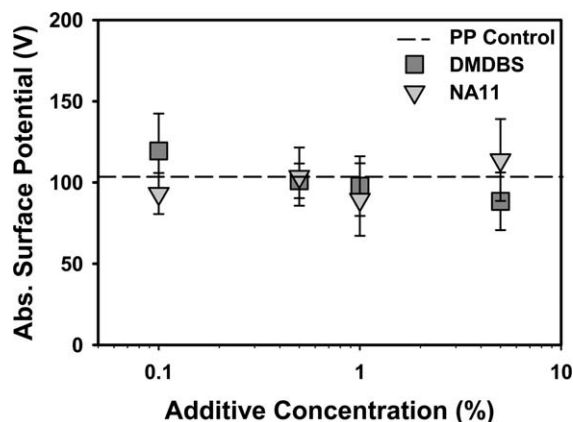

Figure 11. Initial potentials of the nucleating agent containing samples (after charging 1 min under 4.5 kV/cm corona discharger).
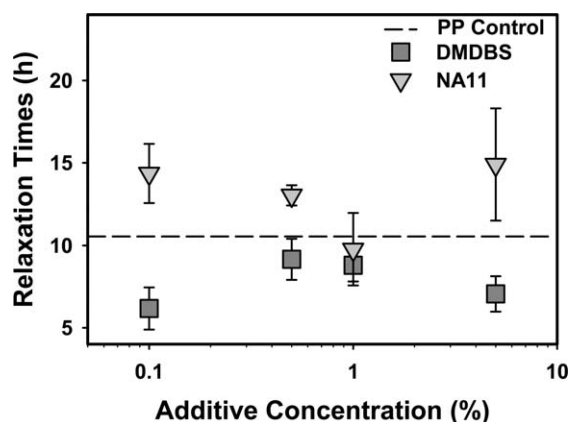

Figure 12. The relaxation times of the samples containing nucleating agents (obtained from ISPD graphs).
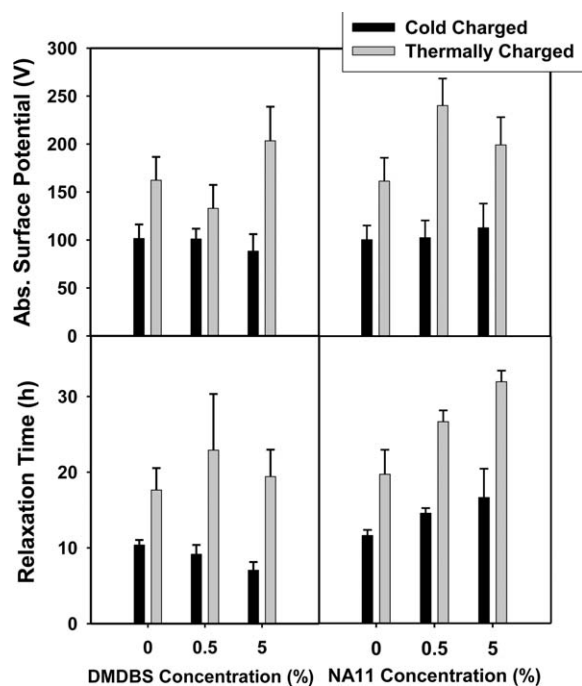
Figure 13. Initial potentials and relaxation times of thermally charged samples. (C) indicates cold charged, whereas (T) indicates thermally charged.

Another interesting finding here is that the charge decay for filaments appears to be faster than those reported for nucleated films.[13–15,18–20] Filaments have a significantly higher surface area compared to films and therefore, charge decay in the filaments might be surface dependent—this needs to be studied further.

CONCLUSIONS

The morphological and electret behavior of PP filaments containing nucleating agents were examined. The crystal structure remained relatively unchanged with the addition of nucleating agents. The initial potential for cold charged samples was not enhanced significantly. Thermal charging improved electret properties, which can be attributed to the softening of the polymer, improved corona conditions, and the activation of polarizable species due to enhanced charge carrier mobility at elevated temperatures. The enhancement in charging properties is significant; polarization of additive molecules is thought to be most important factor responsible for this enhancement.

ACKNOWLEDGMENTS

REFERENCES

1. Sessler, G. M.; West, J. E. *J. Acoust. Soc. Am.* **1973**, *53*, 1589.

2. Silva, M. D.; Bandeira, I. N.; Miranda, L. C. M. *J. Phys. E: Sci. Inst.* **1987**, *20*, 1476.

3. Klaase, P. T.; Van Turnhout, J. US Patent No. 4,588,537, **1986**.

4. R. G. Brown, US Patent No. 3,487,610, **1970**.

5. R. C. Brown, Air Filtration; Pergamon Press: Oxford, **1993**.

6. Raynor, P. C.; Kim, B. G.; Ramachandran, G.; Strommen, M. R.; Horns, J. H.; Streifel, A. J. *Indoor Air* **2008**, *18*, 51.

7. Turkevich, L. A.; Myers, D. L. US Patent No. 6,162,535, **2000**.

8. Rousseau, A. D.; Jones, M. E.; Mei, B. Z. US Patent No. 6,238,466, **2001**.

9. Rousseau, A. D.; Jones, M. E.; Mei, B. Z. US Patent No. 6,068,799, **2000**.

10. Jones, M. E.; Rousseau, A. D. US Patent No. 5,472,481, **1995**.

11. Jones, M. E.; Rousseau, A. D. US Patent No. 5,411,576, **1995**.

12. Huberty, J. S. US Patent No. 6,627,563, **2003**.

13. Behrendt, N.; Altstadt, V.; Schmidt, H.W.; Zhang, X.; Sessler, G. M. *IEEE Trans.* **2006**, *13*, 992.

14. Mohmeyer, N.; Behrendt, N.; Zhang, X.; Smith, P.; Altstadt, V.; Sessler, G. M.; Schmidt, H. W. *Polymer* **2007**, *48*, 1612.

15. Hillenbrand, J.; Behrendt, N.; Mohmeyer, N.; Altstadt, V.; Schmidt, H. W.; Sessler, G. M. *Electrets, ISE-12 12th International Symposium,* **2005**; pp 276–279.

16. Behrendt, N.; Mohmeyer, N.; Hillenbrand, J.; Klaiber, M.; Zhang, X.; Sessler, G. M.; Schmidt, H. W.; Altstadt, V. *J. Appl. Polym. Sci.* **2006**, *99*, 650.

17. Hillenbrand, J.; Behrendt, N.; Altstadt, V.; Schmidt, H. W.; Sessler, G. M. *J. Phys. D: Appl. Phys.* **2006**, *39*, 535.

18. Mohmeyer, N.; Schmidt, H. W.; Kristiansen, P. M.; Altstadt, V. *Macromolecules* **2006**, *39*, 5760.

19. Mohmeyer, N.; Müller, B.; Behrendt, N.; Hillenbrand, J.; Klaiber, M.; Zhang, X.; Smith, P.; Altstadt, V.; Sessler, G. M.; Schmidt, H.-W. *Polymer* **2004**, *45*, 6655.

20. Erhard, D.; Lovera, D.; von Salis-Soglio, C.; Giesa, R.; Altstadt, V.; Schmidt, H. W. Complex Macromolecular Systems II, *Adv. Polym. Sci.* **2010**, *228*, 155.

21. Blythe, A. R.; Bloor, D. Electrical Properties of Polymers; Cambridge University Press: New York, **2005**; pp 85.

22. Cheng, S. Z. D.; Janimak, J. J.; Zhang, A.; Hsieh, E. T. *Polymer* **1991**, *32*, 648.

23. Salem, D. R. Structure Formation in Polymeric Fibers; Hanser Verlag: München, **2001**; p 461.

24. Kilic, A.; Shim, E.; Yeom, B. Y.; Pourdeyhimi, B. *J. Electrostat.* **2013**, *71*, 41.

25. Groh, W.; Macholdt, H. T.; Gibson, B. D.; Walden, J. R.; Felton, C. D. US Patent No. 5,558,809, **1996**.

26. Kristiansen, M.; Werner, M.; Tervoort, T.; Smith, P.; Blomenhofer, M.; Schmidt, H. W. *Macromolecules* **2003**, *36*, 5150.

27. Lilaonitkul, A.; Cooper, S. L. *Macromolecules* **1979**, *12*, 1146.

28. Nalwa, H. S. Ferroelectric Polymers: Chemistry, Physics, and Applications; CRC Press: New York, **1995** pp 207–211.